

Supporting Information

Zn₃V₂O₇(OH)₂(H₂O)₂ and Zn₃V₂O₈ Nanostructure: Controlled Fabrication and Photocatalytic Performance

Rui Shi¹, Yajun Wang¹, Feng Zhou² and Yongfa Zhu^{1}*

¹ Department of Chemistry, Tsinghua University, Beijing, 100084, China

² Department of Materials Science and Engineering, Dalian Maritime University, Dalian 116026,
P. R. China

Corresponding author. E-mail: zhuyf@tsinghua.edu.cn; Fax: +86-10-62787601; Tel:

+86-10-62787601.

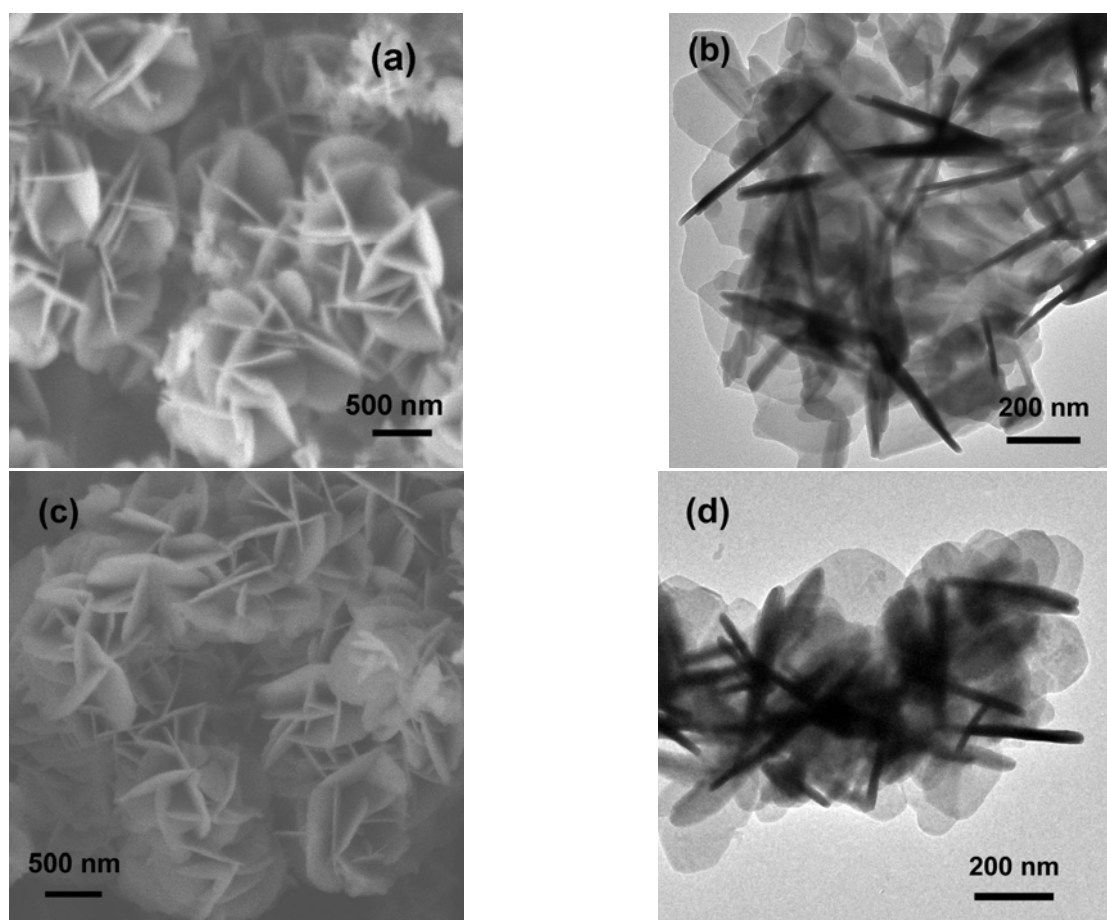


Fig. S1. SEM images (a), TEM images (b) of $\text{Zn}_3\text{V}_2\text{O}_7(\text{OH})_2(\text{H}_2\text{O})_2$ prepared at 70 °C, SEM images (c), TEM images (d) of $\text{Zn}_3\text{V}_2\text{O}_7(\text{OH})_2(\text{H}_2\text{O})_2$ prepared at 80 °C.

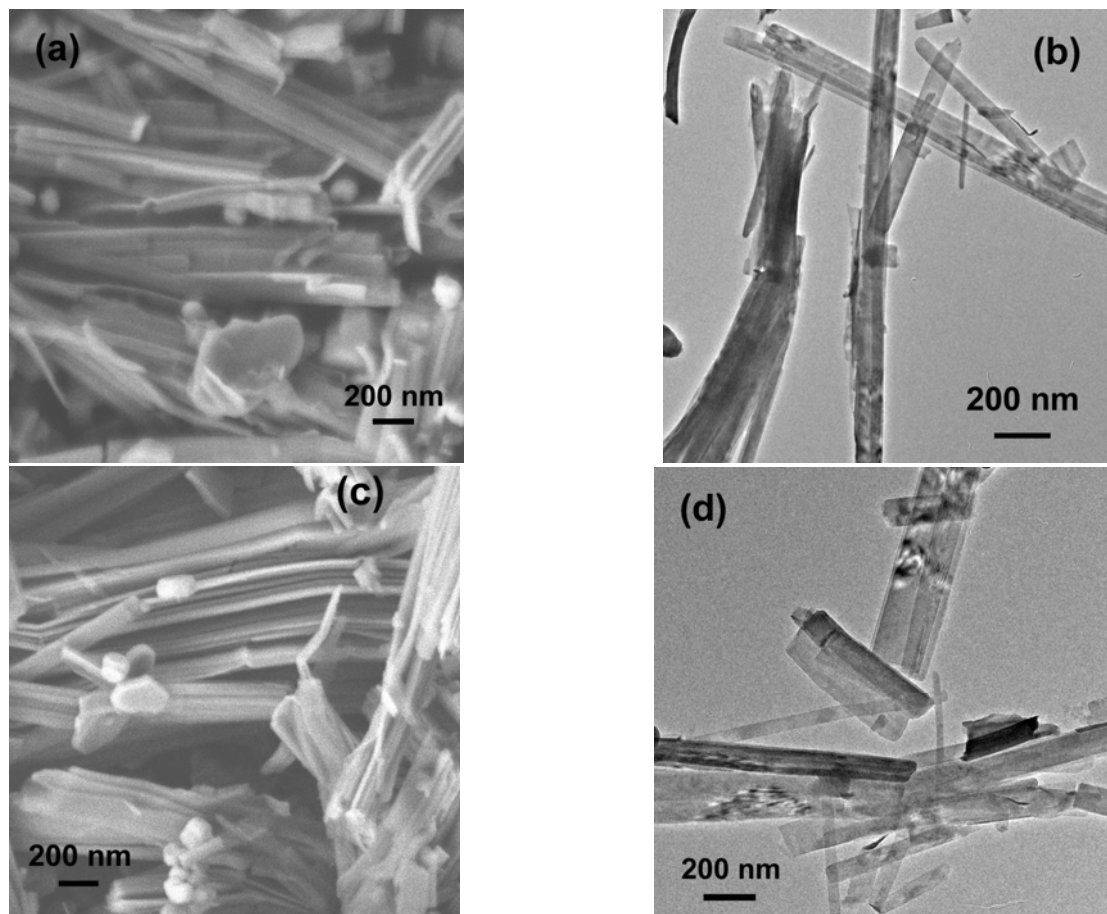


Fig. S2. SEM images (a), TEM images (b) of $\text{Zn}_3\text{V}_2\text{O}_7(\text{OH})_2(\text{H}_2\text{O})_2$ prepared at 120 °C, SEM images (c), TEM images (d) of $\text{Zn}_3\text{V}_2\text{O}_7(\text{OH})_2(\text{H}_2\text{O})_2$ prepared at 140 °C.

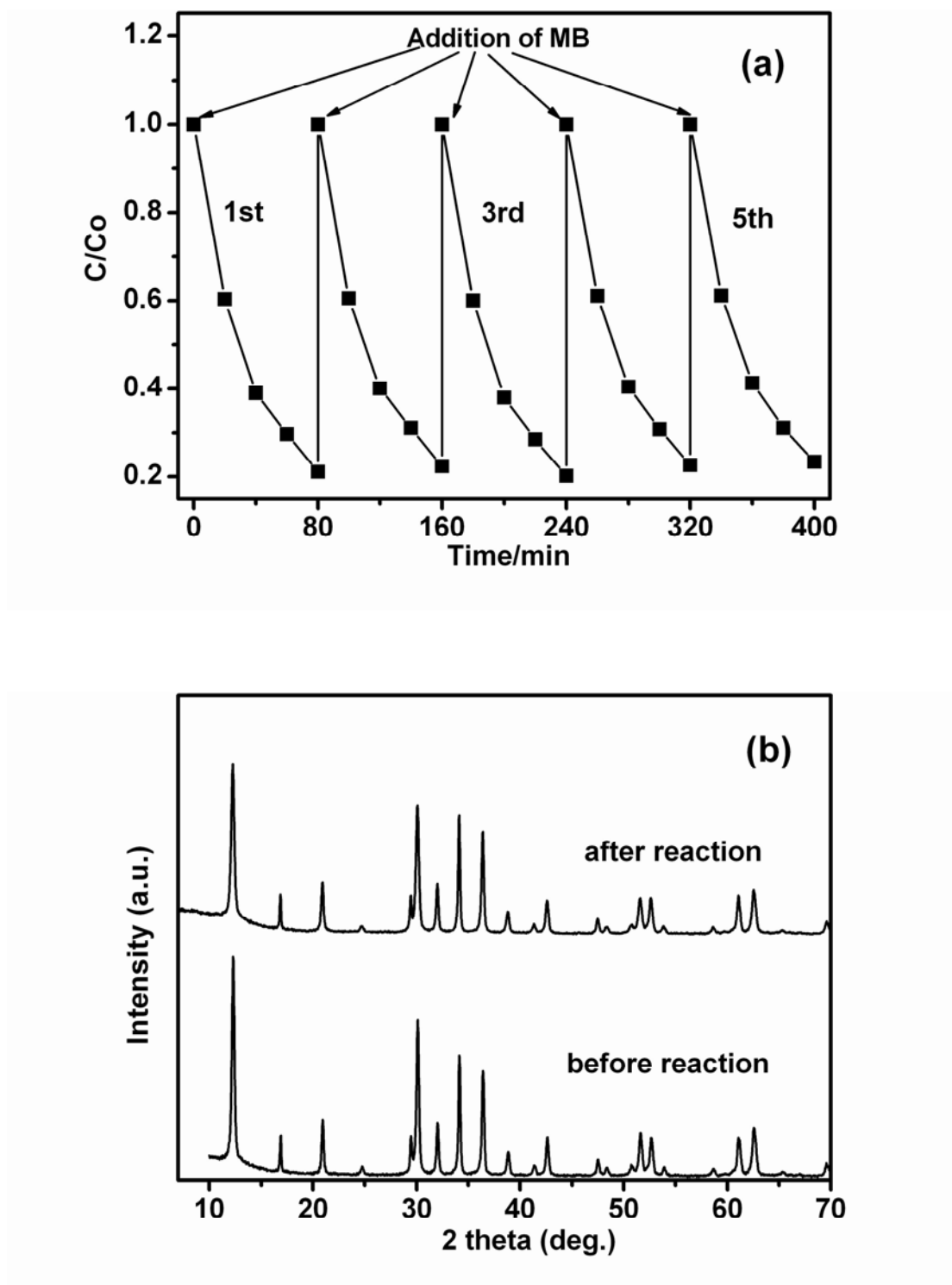


Fig. S3. (a) Evaluation of durability of $Zn_3V_2O_7(OH)_2(H_2O)_2$ photocatalytic degradation from the repeatable degrading of MB under UV light irradiation. (b) XRD patterns of $Zn_3V_2O_7(OH)_2(H_2O)_2$ before and after MB degrading.

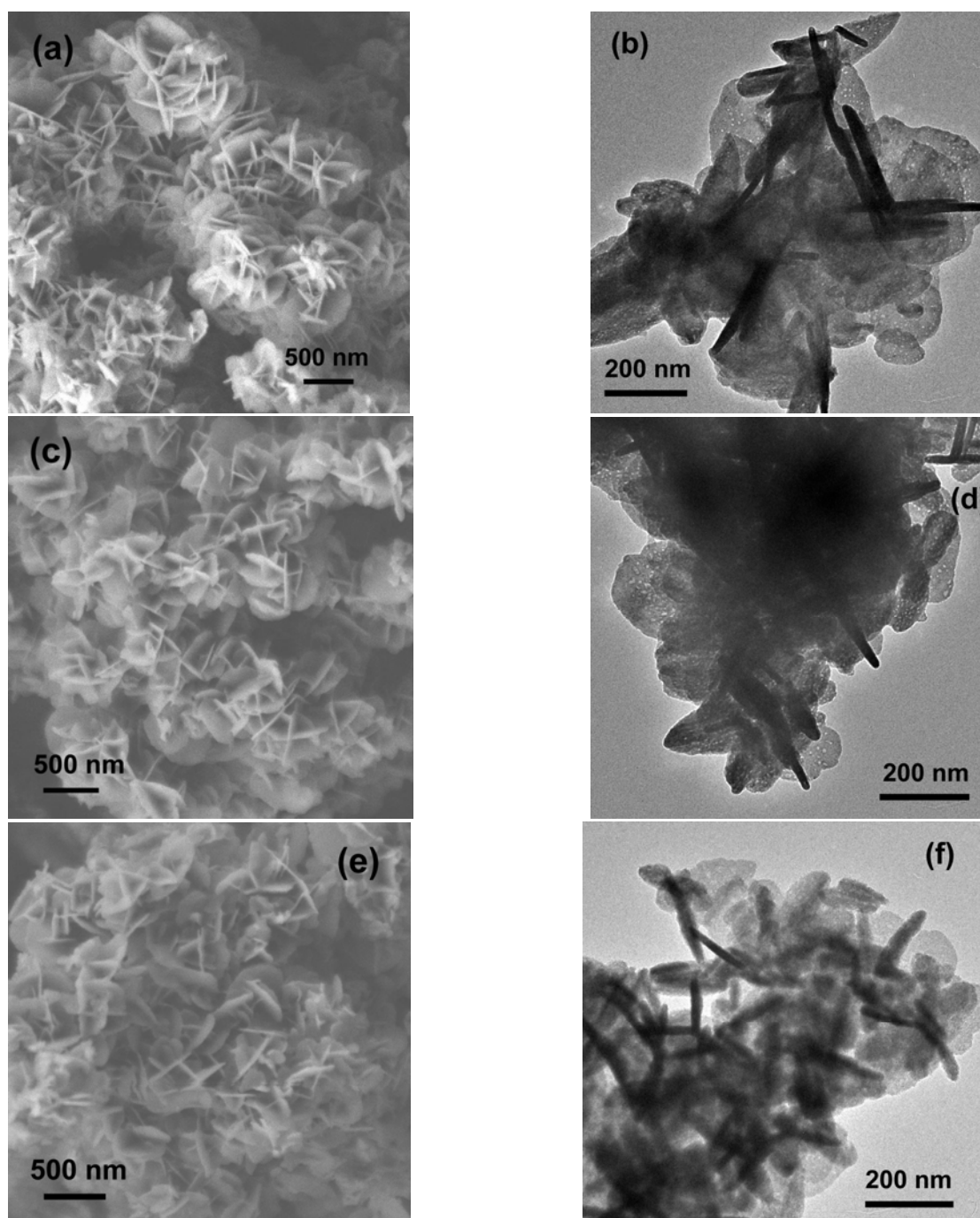
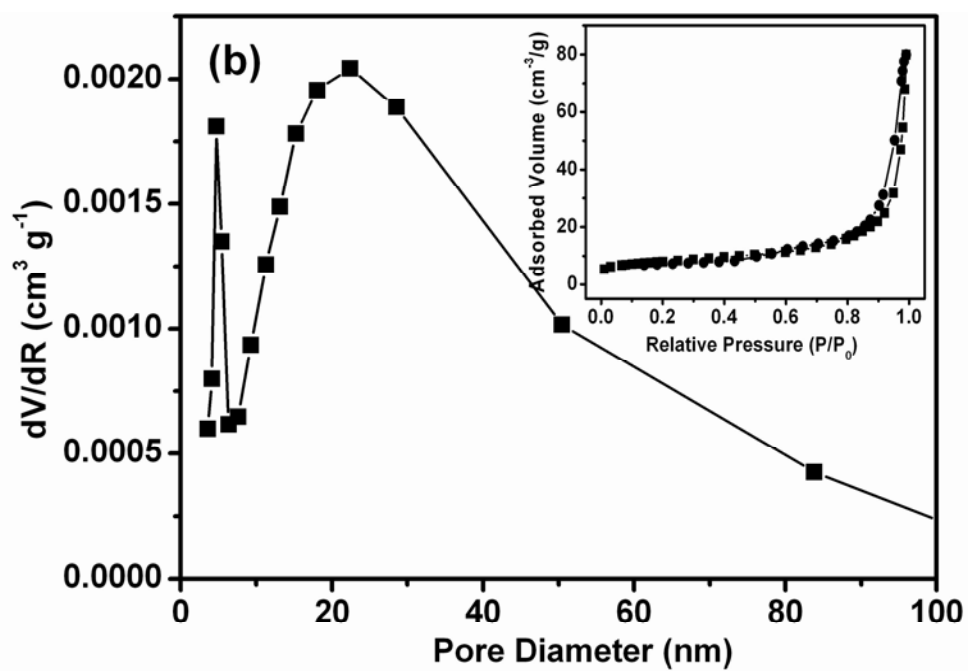
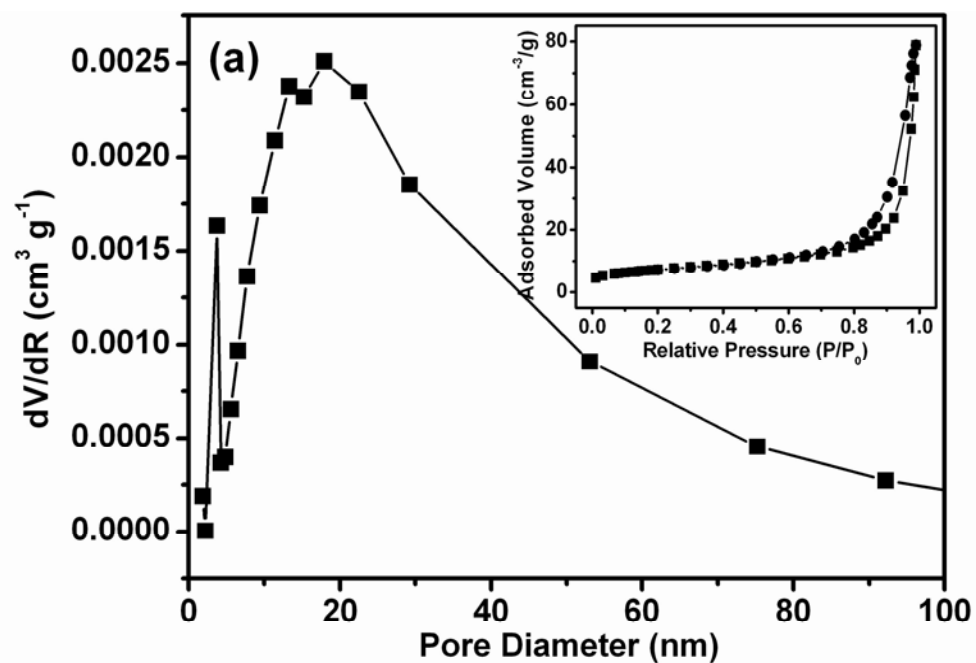


Fig. S4. SEM images (a), TEM images (b) of $\text{Zn}_3\text{V}_2\text{O}_8$ calcinated at 350 °C, SEM images (c), TEM images (d) of $\text{Zn}_3\text{V}_2\text{O}_8$ calcinated at 400 °C, SEM images (e), TEM images (f) of $\text{Zn}_3\text{V}_2\text{O}_8$ calcinated at 450 °C.



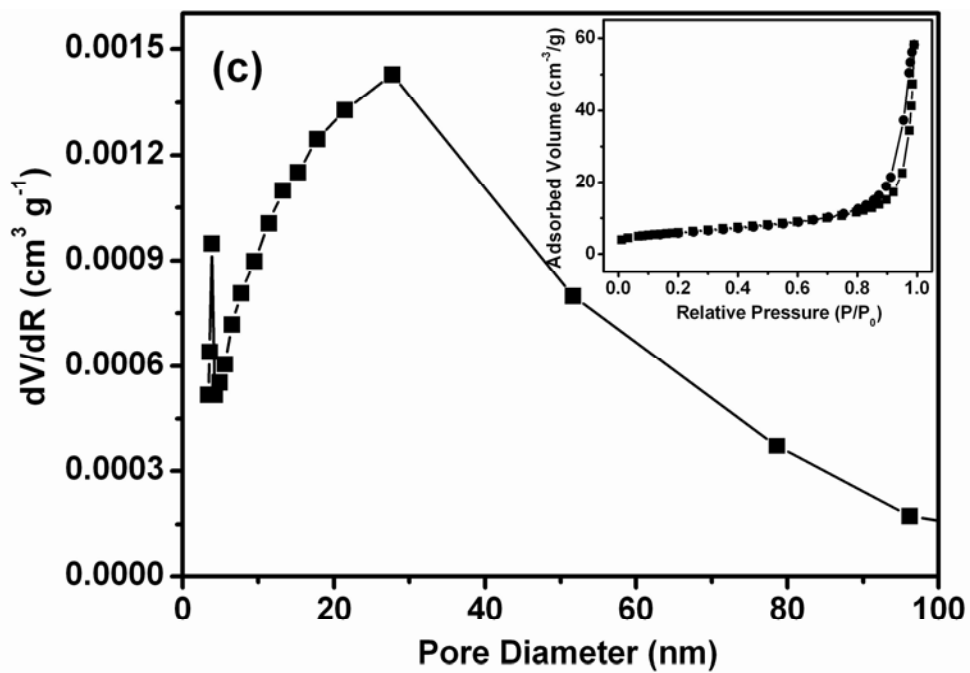


Fig. S5. N_2 adsorption-desorption isotherms (inset) and Barret-Joyner-Halenda (BJH) pore size distribution plots of the (a) $\text{Zn}_3\text{V}_2\text{O}_8$ calcinated at 350°C , (b) $\text{Zn}_3\text{V}_2\text{O}_8$ calcinated at 400°C , (c) $\text{Zn}_3\text{V}_2\text{O}_8$ calcinated at 450°C ,

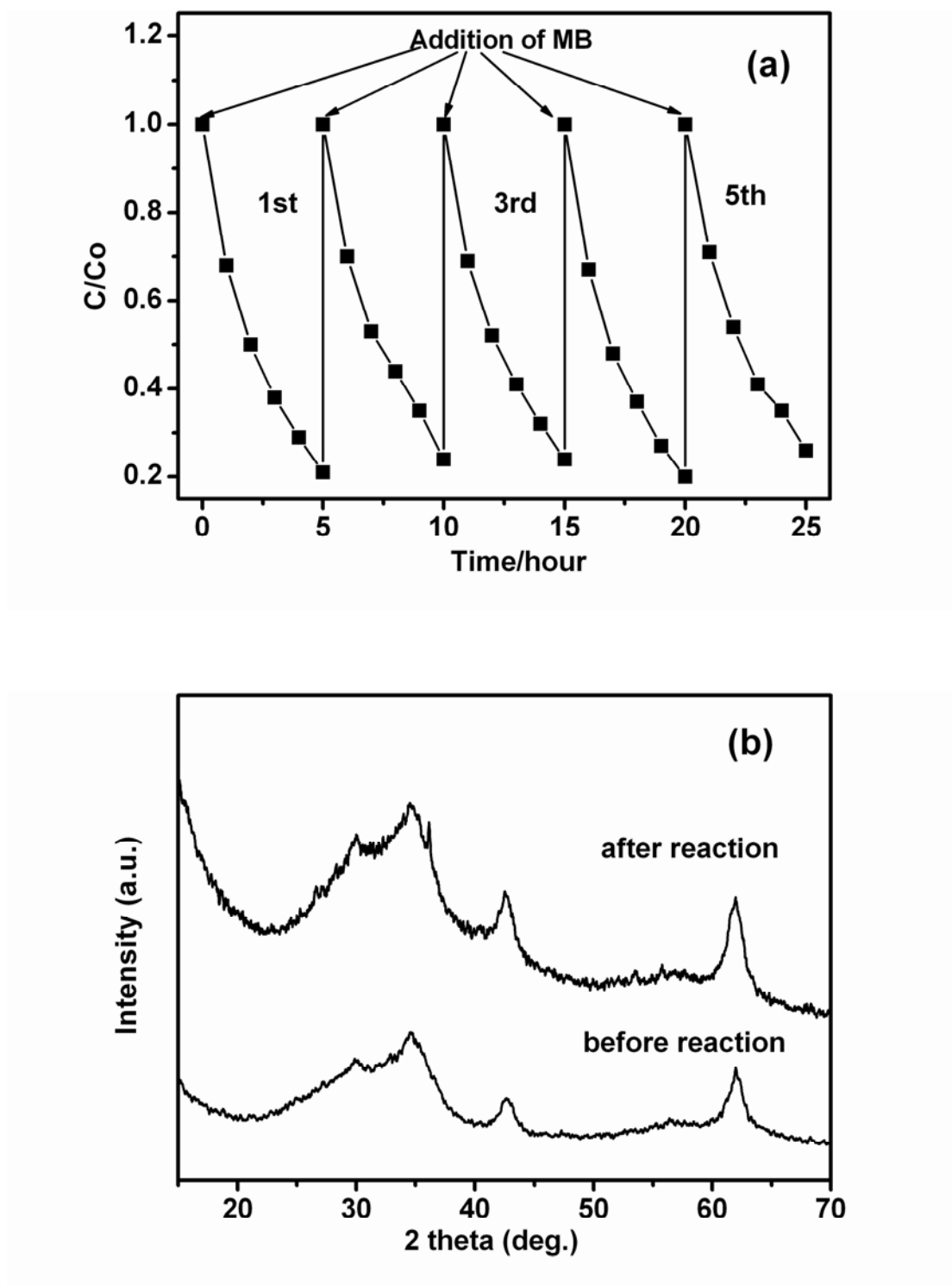


Fig. S6. (a) Evaluation of durability of $Zn_3V_2O_8$ photocatalytic degradation from the repeatable degrading of MB under visible-light irradiation ($\lambda > 420\text{nm}$). (b) XRD patterns of $Zn_3V_2O_8$ before and after MB degrading.

The peaks at 5.2 min assigned to MB. During the course of the photocatalytic oxidation of MB, a series of new signals appeared, whereas the characteristic signals of MB disappeared. To examine the process in detail, the intermediates were further identified by LC/MS. The suggested structures of the intermediates were shown in Table S1. All of these indicated that the destruction of the conjugated structure of MB occurred in the suspensions during the course of irradiation.

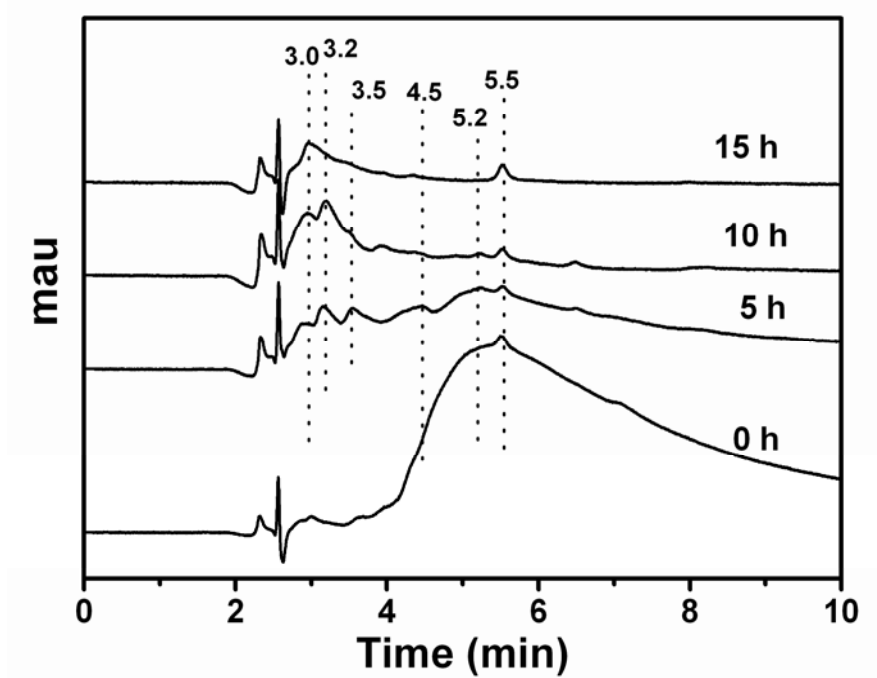
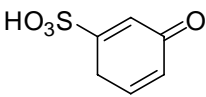
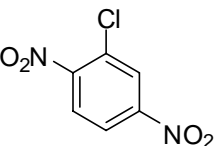
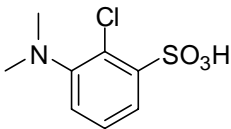
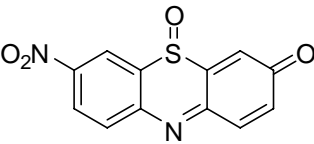
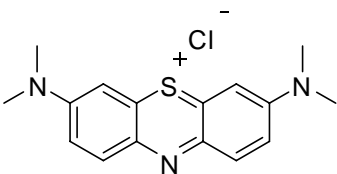


Fig. S7. Chromatograms of MB degradation products with the initial concentration of 5.0×10^{-5} mol L⁻¹.

TABLE S1. Suggested Structures for the Intermediates based on LC-MS Results.

Retention time (t_R , min)	Structure formula	Molecular Weight
3.0		174
3.2		202
3.5		235
4.5		274
5.2		320

In order to exclude the self-sensitization effect of methylene blue, 4-chlorophenol was used to test the photocatalytic activity of the as-prepared samples. The concentration variation of 4-chlorophenol was examined by HPLC. The Fig. S8 and Fig. S9 show the degradation of 4-chlorophenol over $\text{Zn}_3\text{V}_2\text{O}_7(\text{OH})_2(\text{H}_2\text{O})_2$ and $\text{Zn}_3\text{V}_2\text{O}_8$ powders. We can see that 4-chlorophenol could be well degraded, which suggest that the degradation of organic contamination was not due to self-sensitization but due to photocatalytic reaction.

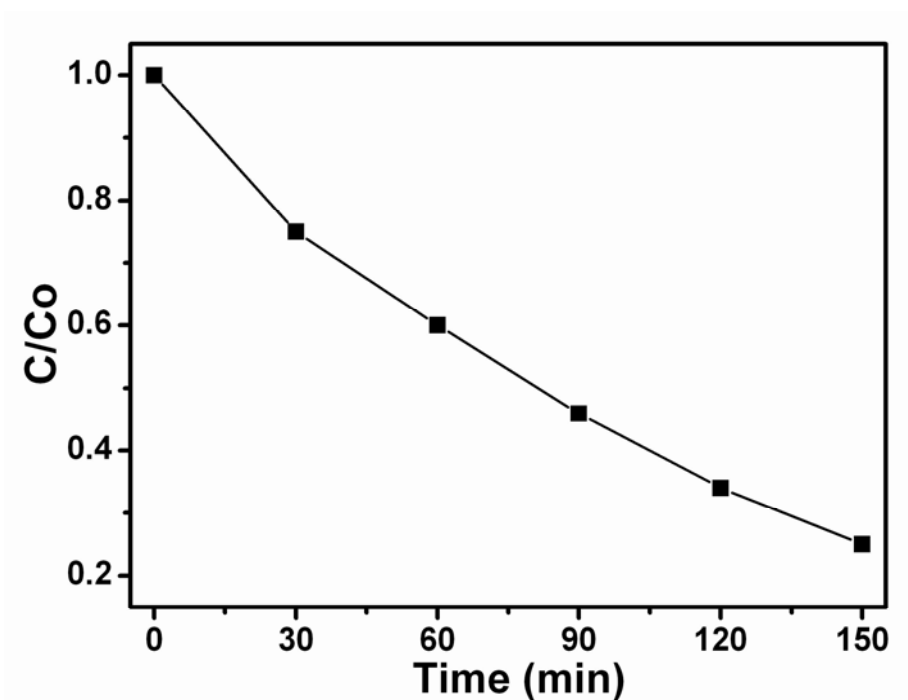


Fig. S8 Photocatalytic 4-chlorophenol degradation under UV light irradiation over $\text{Zn}_3\text{V}_2\text{O}_7(\text{OH})_2(\text{H}_2\text{O})_2$ prepared 70 °C hydrothermal temperature.

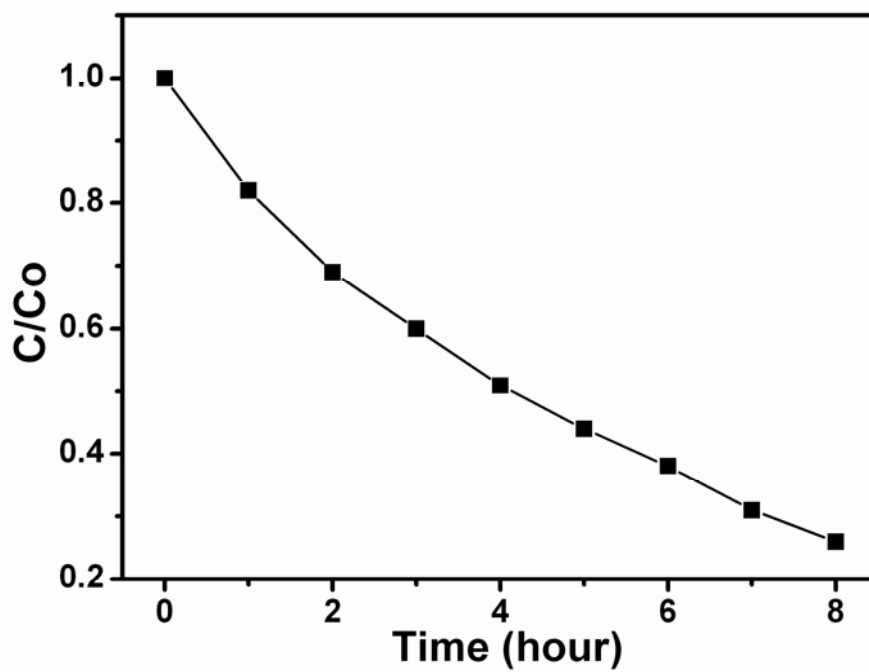


Fig. S9 Photocatalytic 4-chlorophenol degradation under visible light irradiation ($\lambda > 420$ nm) over $\text{Zn}_3\text{V}_2\text{O}_8$ calcinated at 300°C